JACC: ADVANCES VOL. 2, NO. 10, 2023

ORIGINAL RESEARCH

HEART FAILURE AND CARDIOMYOPATHIES

Obesity-Related Differences in Pathomechanism and Outcomes in Patients With HFpEF

A CMR Study

Shiro Nakamori, MD,[a,b] Selcuk Kucukseymen, MD,[a] Jennifer Rodriguez, BS,[a] Forough Yazdanian, MD,[a] Long H. Ngo, PhD,[a] Deepa M. Gopal, MD, MS,[c] Warren J. Manning, MD,[a,d] Reza Nezafat, PhD[a]

ABSTRACT

BACKGROUND Clinical significance of an integrated evaluation of epicardial adipose tissue (EAT) and the right ventricle (RV) in heart failure with preserved ejection fraction (HFpEF) is unknown.

OBJECTIVES The authors investigated the potential of EAT and RV quantification for obesity-related pathophysiology and risk stratification in obese HFpEF patients using cardiovascular magnetic resonance (CMR).

METHODS A total of 150 patients (obese, body mass index ≥30 kg/m^2; n = 73, nonobese, body mass index <30 kg/m^2; n = 77) with a clinical diagnosis of HFpEF undergoing CMR were retrospectively identified. EAT volume surrounding both ventricles were quantified with manual delineation on cine images. Total RV volume (TRVV) was calculated as the sum of RV cavity and mass at end-diastole. The endpoint was the composite of all-cause mortality and first HF hospitalization.

RESULTS During a median follow-up of 46 months, 39 nonobese patients (51%) and 32 obese patients (44%) experienced the endpoint. EAT was a prognostic biomarker regardless of obesity and was independently correlated with TRVV. In obese HFpEF, EAT correlated with RV longitudinal strain (r = 0.32, P = 0.006), and increased amount of EAT and TRVV was associated with greater left ventricular end-diastolic eccentric index (r = 0.36, P = 0.002). The integration of RV quantification into EAT provided improved risk stratification with a C-statistic increase from 0.70 to 0.79 in obese HFpEF. Obese patients with EAT<130 ml and TRVV<180 ml had low risk (annual event rate 3.2%), while those with increased EAT ≥130 ml and TRVV ≥180 ml had significantly higher risk (annual event rate 11.8%; P < 0.001).

CONCLUSIONS CMR quantification of EAT and RV structure provides additive risk stratification for adverse outcomes in obese HFpEF. (JACC Adv 2023;2:100730) © 2023 The Authors. Published by Elsevier on behalf of the American College of Cardiology Foundation. This is an open access article under the CC BY-NC-ND license (http://creativecommons.org/licenses/by-nc-nd/4.0/).

From the [a]Department of Medicine, Beth Israel Deaconess Medical Center and Harvard Medical School, Boston, Massachusetts, USA; [b]Department of Cardiology and Nephrology, Mie University Graduate School of Medicine, Tsu, Mie, Japan; [c]Cardiovascular Division, Department of Medicine, Boston University School of Medicine, Boston, Massachusetts, USA; and the [d]Department of Radiology, Beth Israel Deaconess Medical Center and Harvard Medical School, Boston, Massachusetts, USA.

The authors attest they are in compliance with human studies committees and animal welfare regulations of the authors' institutions and Food and Drug Administration guidelines, including patient consent where appropriate. For more information, visit the Author Center.

Manuscript received April 6, 2023; revised manuscript received August 17, 2023, accepted September 19, 2023.

ISSN 2772-963X https://doi.org/10.1016/j.jacadv.2023.100730

ABBREVIATIONS AND ACRONYMS

BMI = body mass index

CMR = cardiovascular magnetic resonance

EAT = epicardial adipose tissue

FWLS = free wall longitudinal strain

GLS = global longitudinal strain

HF = heart failure

HFpEF = heart failure with preserved ejection fraction

RV = right ventricular

THV = total heart volume

TRVV = total right ventricular volume

Heart failure (HF) with preserved ejection fraction (HFpEF) is a heterogeneous clinical syndrome with symptoms and signs of HF and normal or near-normal left ventricular (LV) ejection fraction (LVEF).[1-4] HFpEF accounts for half as many as symptomatic HF, and its prevalence relative to HF with reduced ejection fraction continues to rise at a rate of 1% per year.[5] However, successful therapeutic approaches are limited to treatment with sodium-glucose cotransporter-2 inhibitors, neurohumoral antagonists, or mineralocorticoid receptor antagonists, and angiotensin receptor-neprilysin inhibitors in certain subgroups of HFpEF.[6,7] This therapeutic failure is attributed to the pathophysiological diversity of HFpEF.[4,8] Thus, more precise phenotyping of HFpEF patients is a major unmet clinical need which is being investigated using different approaches including clinical, genetic, proteomics, and blood biomarkers.[9-13]

More than 80% of HFpEF patients are overweight or obese in the United States.[14] Studies have shown larger right ventricular (RV) volume and mass in overweight or obese patients without overt heart disease.[15,16] Epicardial adipose tissue (EAT), which is often increased in obesity, promotes myocardial inflammation and fibrosis via local secretion of proinflammatory cytokines[17] and was associated with adverse prognosis in HF patients with LVEF >40%.[18] In addition, enlarged EAT may develop abnormal ventricular-adipose interactions (ie, pericardial restraint) within a fixed pericardial space, indicating a unique phenotype in obese HFpEF.[12,19] However, the relationship between EAT and RV morphology in obesity-related HFpEF patients is not well studied. Accordingly, we sought to unravel the obesity-related characteristics in pathomechanism and outcomes in HFpEF patients and the potential of an integrated assessment of EAT and RV morphology using cardiovascular magnetic resonance (CMR) for enhanced clinical phenotyping and risk stratification in obesity-related HFpEF patients.

METHODS

STUDY POPULATION. We retrospectively identified 204 consecutive patients with a clinical diagnosis of HFpEF referred for clinical CMR. Subjects were identified by querying the Beth Israel Deaconess Medical Center clinical CMR report database and electronic medical records from April 2006 to January 2018. Exclusion criteria were: 1) LVEF <50%; 2) hypertrophic, inflammatory, infiltrative, arrhythmogenic cardiomyopathies, and constrictive pericarditis; 3) more than moderate valvular heart disease, pulmonary disease defined as radiographically severe lung disease, and chronic kidney disease (estimated glomerular filtration rate <30 ml/min/1.73 m^2); 4) previous cardiac surgery. HFpEF was diagnosed according to current HF guidelines: 1) symptoms ± signs; 2) elevated levels of B-type natriuretic peptide; 3) relevant structural heart disease including LV hypertrophy and/or left atrial (LA) enlargement, and/or evidence of diastolic dysfunction on echocardiography.[20,21] All HF subjects underwent CMR study and transthoracic echocardiography, and there were no intervening procedures. Patient demographics and clinical follow-up records from the hospital electronic medical records were reviewed. Laboratory testing and electrocardiogram performed within 15 days of scan were obtained, and HF signs/symptoms were collected at the time of scan. The study was carried out with Beth Israel Deaconess Medical Center Institutional Review Board approval, which waived written informed consent for the retrospective study.

CMR IMAGE ACQUISITION. All CMR images were acquired with 1.5-T CMR scanner (Achieva 1.5-T, Philips Medical Systems) equipped with a 5-element or 32-element cardiac coil. The CMR protocol included cine and late gadolinium enhanced (LGE) imaging. To assess LV/RV myocardial function, geometry, and mass, 10 to 12 short-axis stack cine images and 4-chamber long-axis image were acquired using a cine-balanced steady-state free precession sequence (slice thickness, 8 mm; gap, 2 mm; in-plane spatial resolution, 2 × 2 mm; 30 ms temporal resolution). Ten to 20 min after injection of 0.1 to 0.2 mmol/kg of Gd-DTPA (Magnevist, Bayer Schering) or Gd-BOPTA (MultiHance, Bracco Imaging SpA), short- and long-axis 2D inversion recovery LGE images were acquired using a breath-hold, segmented inversion-recovery sequence (8-mm slice thickness, 2-mm interslice gap, TR, 4.2 ms; TE, 1.8 ms; FA, 20°; FOV, 320 × 320 mm^2; matrix, 160 × 160; and spatial resolution of 2 mm^2).

IMAGE ANALYSIS. CMR images were analyzed using commercial workstations (CMR42, version 5.11.1, Circle Cardiovascular Imaging Inc). At end-diastole and end-systole, epi- and endocardial LV borders were manually traced from contiguous short-axis cine images covering the LV apex to mitral valve plane to calculate LV and RV end-diastolic volume and end-systolic volume, stroke volume (SV), and ejection fraction. LV and RV mass were calculated as the sum of the myocardial volume multiplied by the specific

TABLE 1 Clinical Characteristics

	All Patients (N = 150)	Nonobese Patients (n = 77)	Obese Patients (n = 73)	*P* Value
Demographic parameters				
Age, y	65 ± 12	68 ± 13	61 ± 11	0.001
Female	68 (45)	35 (45)	33 (45)	0.98
Race				0.87
White	123 (82)	63 (82)	60 (82)	
Asian	3 (2)	2 (3)	1 (1)	
Black	21 (14)	11 (14)	10 (14)	
Other	3 (2)	1 (1)	2 (3)	
AF presence	36	22 (29)	14 (19)	0.18
Weight, kg	89.9 ± 24.8	74.6 ± 13.9	106.0 ± 23.6	<0.001
Height, cm	170.3 ± 11.1	171.3 ± 10.5	169.3 ± 11.7	0.29
BMI, kg/m^2	30.9 ± 7.9	25.3 ± 3.3	36.9 ± 6.9	<0.001
Comorbidities				
CAD	56 (37)	29 (38)	27 (37)	0.93
Prior MI	21 (14)	14 (18)	7 (10)	0.13
Dyslipidemia	84 (56)	41 (53)	43 (59)	0.49
Diabetes	62 (41)	33 (43)	29 (40)	0.70
Hypertension	88 (59)	41 (53)	47 (64)	0.27
CKD[a]	61 (41)	35 (45)	26 (36)	0.22
Tobacco use	49 (33)	27 (35)	22 (30)	0.52
Obstructive sleep apnea	48 (32)	16 (21)	32 (44)	0.002
Mild valvular diseases	20 (13)	12 (16)	8 (11)	0.40
Anemia[b]	26 (17)	16 (21)	10 (14)	0.25
ECG features				
PR duration, ms	170 ± 33	171 ± 35	168 ± 32	0.57
QRS duration, ms	104 ± 21	101 ± 22	107 ± 21	0.06
QTc duration, ms	444 ± 37	439 ± 29	449 ± 43	0.09
Treatments				
Diuretics	142 (95)	70 (91)	72 (99)	0.03
Beta-blockers	91 (61)	45 (58)	46 (63)	0.57
ACEI/ARB	82 (55)	43 (56)	39 (53)	0.77
Calcium-channel blockers	56 (37)	32 (42)	24 (33)	0.27
Statins	104 (69)	52 (68)	52 (71)	0.62
HF signs/symptoms				
Fatigue/malaise	66 (44)	36 (47)	30 (41)	0.49
Shortness of breath	109 (73)	50 (65)	59 (81)	0.03
Swelling of limb	68 (45)	33 (43)	35 (48)	0.53
Prior HF admission	16 (11)	10 (13)	6 (8)	0.34
Laboratory parameters				
Hb, g/dl	14.5 ± 1.9	14.2 ± 1.9	14.8 ± 1.9	0.05
Glucose, mg/dl	84 ± 37	82 ± 34	86 ± 39	0.47
Creatinine, mg/dl	0.9 ± 0.5	0.9 ± 0.5	0.9 ± 0.5	0.99
Na, mmol/l	133 ± 6	133 ± 6	133 ± 6	0.70
BUN, mg/dl	15 ± 14	16 ± 17	14 ± 10	0.45
NT-pro BNP, pg/ml	1,281 (541-2,580)	1,339 (544-2,481)	1,164 (533-2,815)	0.26
Outcome data				
Primary endpoint	71 (47)	39 (51)	32 (44)	0.40
HF admission	59 (39)	32 (42)	27 (37)	0.57
All-cause death	36 (24)	23 (30)	13 (18)	0.08
Follow-up duration, mo	46 (29-78)	40 (15-75)	52 (35-90)	0.03

Values are mean ± SD, n (%), or median (IQR). [a]CKD is defined as kidney damage or glomerular filtration rate (GFR) <60 mL/min/1.73 m^2. [b]Anemia is defined as hemoglobin <13 g/dL in men and <12 g/dL in women.

ACEI/ARB = angiotensin-converting enzyme inhibitors/angiotensin-receptor blockers; AF = atrial fibrillation; BMI = body mass index; CAD = coronary artery disease; CKD = chronic kidney disease; DM = diabetes mellitus; HF = heart failure; HTN = hypertension; MI = myocardial infarction; NT-pro BNP = N-terminal pro B-type natriuretic peptide.

TABLE 2 Cardiac Performance, CMR, and Echocardiographic Measurements

	All Patients (N = 150)	Nonobese Patients (n = 77)	Obese Patients (n = 73)	*P* Value
Hemodynamic parameters				
Systolic BP, mm Hg	127 ± 19	124 ± 20	130 ± 17	0.06
Diastolic BP, mm Hg	70 ± 12	68 ± 12	72 ± 12	0.07
Heart rate, beats/min	79 ± 14	79 ± 14	79 ± 15	0.7
E_{es}, mm Hg/ml	2.0 ± 1.1	2.0 ± 1.1	2.0 ± 1.2	0.92
Stroke work, mm Hg·ml	8,142 ± 2,707	7,542 ± 2,676	8,774 ± 2,611	0.005
E_a, mm Hg/ml	1.4 ± 0.4	1.4 ± 0.4	1.3 ± 0.5	0.4
E_a/E_{es}	0.83 ± 0.38	0.83 ± 0.33	0.83 ± 0.43	0.97
SVR, dyne·s^{-1} cm^{-5}	1,105 ± 413	1,120 ± 375	1,089 ± 452	0.65
Arterial compliance, ml/mm Hg	1.7 ± 0.7	1.7 ± 0.7	1.8 ± 0.7	0.35
CPO, W/100g	1.3 ± 0.4	1.3 ± 0.5	1.2 ± 0.4	0.17
CMR parameters				
LV EDD, mm	53.8 ± 6.9	52.6 ± 7.2	55.0 ± 6.4	0.03
LV EDD index, mm/m^2	26.8 ± 3.9	27.8 ± 3.8	25.7 ± 3.8	<0.001
LV ESD, mm	36.9 ± 15.4	35.8 ± 7.6	38.0 ± 20.3	0.49
AS wall thickness, mm	9.9 ± 2.8	9.4 ± 2.7	10.3 ± 2.7	0.04
IL wall thickness, mm	8.5 ± 2.3	8.1 ± 2.2	8.8 ± 2.4	0.06
LV mass, g	108.3 ± 33.1	101.6 ± 28.9	115.4 ± 35.8	0.01
LV mass index, g/m^2	53.4 ± 14.9	53.6 ± 14.7	53.3 ± 15.3	0.92
LV EDV, ml	157.2 ± 43.2	151.9 ± 42.7	162.9 ± 43.3	0.12
LV EDV index, ml/m^2	76.7 ± 22.4	77.8 ± 22.7	75.7 ± 22.1	0.57
LV ESV, ml	63.9 ± 27.0	62.0 ± 26.5	66.0 ± 27.6	0.37
LV EF, %	60.1 ± 7.3	59.3 ± 6.3	61.0 ± 8.1	0.16
LV stroke volume, ml	91.0 ± 26.2	86.0 ± 24.7	96.2 ± 26.9	0.02
LV cardiac output, ml/min	7,162 ± 2,355	6,805 ± 2,167	7,540 ± 2,498	0.06
LV eccentric index (diastolic)	1.10 ± 0.09	1.10 ± 0.08	1.11 ± 0.09	0.28
LV eccentric index (systolic)	1.05 ± 0.08	1.04 ± 0.08	1.05 ± 0.09	0.49
LGE presence	32 (21)	25 (32)	7 (10)	<0.001
RV EDV, ml	150.5 ± 42.4	141.4 ± 42.9	160.2 ± 39.8	0.006
RV EDV index, ml/m^2	74.5 ± 19.3	74.3 ± 20.6	74.7 ± 17.9	0.9
RV ESV, ml	64.2 ± 28.1	60.3 ± 26.2	68.3 ± 29.6	0.08
RV EF, %	58.1 ± 9.7	58.1 ± 9.7	58.1 ± 9.7	0.99
RV mass, g	27.9 ± 19.0	27.7 ± 18.0	28.0 ± 20.2	0.91
RV stroke volume, ml	86.5 ± 25.5	81.0 ± 25.8	92.2 ± 24.1	0.007
TRVV, ml	174 ± 47	165 ± 49	183 ± 43	0.02
EAT, ml	123 ± 47	109 ± 37	138 ± 52	<0.001
EAT index, ml/m^2	60 ± 20	57 ± 18	63 ± 21	0.04
THV, ml	557 ± 129	523 ± 122	593 ± 126	<0.001
LV GRS, %	25.0 ± 8.5	26.0 ± 8.4	24.0 ± 8.4	0.15
LV GCS, %	−15.5 ± 3.8	−15.8 ± 3.8	−15.2 ± 3.8	0.39
LV GLS, %	−13.5 ± 3.4	−13.8 ± 3.3	−13.1 ± 3.4	0.17
RV FWLS, %	−18.0 ± 5.1	−18.1 ± 5.3	−17.9 ± 5.0	0.8
LA diameter (PLX), mm	42.6 ± 8.9	42.5 ± 9.3	42.7 ± 8.6	0.88
LA length (4ch), mm	60.9 ± 9.7	60.5 ± 10.4	61.3 ± 9.0	0.6
LA length (2ch), mm	58.7 ± 12.4	57.2 ± 13.1	60.6 ± 11.4	0.17
RA diameter, mm	57.1 ± 9.7	57.0 ± 10.6	57.2 ± 8.7	0.9
LA strain, %	15.8 ± 8.9	15.8 ± 8.8	15.8 ± 9.0	0.99
Echo parameters				
LA dimension, mm	44.9 ± 7.9	43.9 ± 8.2	45.8 ± 7.5	0.15
E wave, cm/s	97 ± 29	98 ± 30	97 ± 29	0.82
Mean e'	7.2 ± 2.6	6.9 ± 2.6	7.5 ± 2.6	0.25
E/e' ratio	12.7 ± 4.8	13.1 ± 5.2	12.2 ± 4.3	0.3
DCT, ms	203 ± 62	201 ± 58	205 ± 67	0.73
ePASP, mm Hg	33 ± 12	33 ± 12	34 ± 12	0.54

Values are mean ± SD or n (%).

AS = anteroseptal; BP = blood pressure; CPO = cardiac power output; DCT = deceleration time; Ea = arterial elastance; EAT = epicardial adipose tissue; EDD = end-diastolic diameter; EDV = end-diastolic volume; Ees = left ventricular end-systolic elastance; EF = ejection fraction; ePASP = estimating pulmonary artery systolic pressure; ESD = end-systolic diameter; ESV = end-systolic volume; FWLS = free wall longitudinal strain; GCS = global circumferential strain; GLS = global longitudinal strain; GRS = global radial strain; HR = heart rate; IL = inferolateral; LA = left atrial; LGE = late gadolinium enhancement; LV = left ventricular; RA = right atrial; RV = right ventricular; SVR = systemic vascular resistance; TRVV = total right ventricular volume at end-diastole.

FIGURE 1 Association of EAT to LV/RV Strain

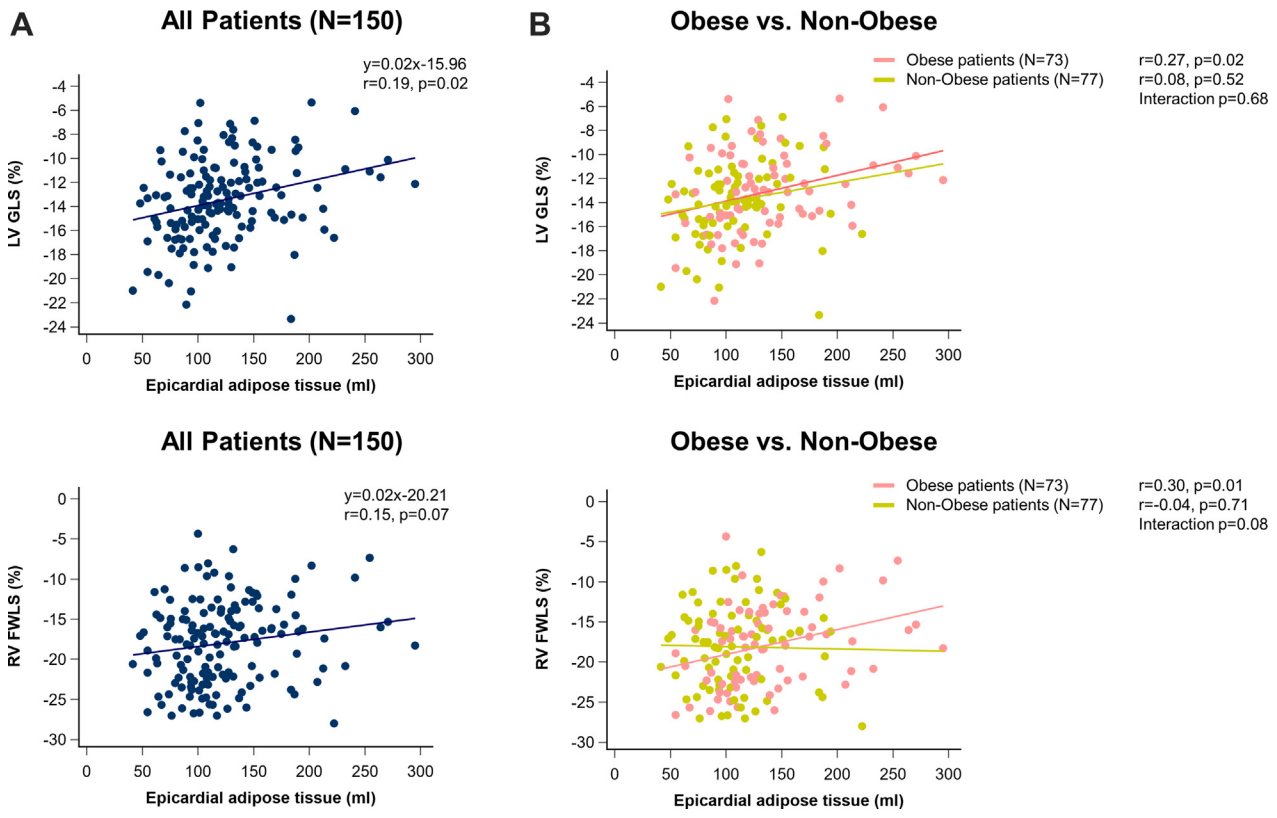

(A) LV GLS as well as RV FWLS mildly correlated with EAT (partial correlation coefficient, r = 0.19, *P* = 0.02, and r = 0.15, *P* = 0.07, respectively). (B) This trend appeared to be more profound in obese cohort (partial correlation coefficient, 0.27 and 0.30, respectively). EAT = epicardial adipose tissue; LV GLS = left ventricular global longitudinal strain; RV FWLS = right ventricular free wall longitudinal strain.

gravity (1.05 g/mL) of myocardial tissue. Ventricular EAT was manually delineated on the end-diastolic short-axis slices, working from the mitral valve annulus towards the most apical slice around the ventricles, and was defined as the adipose tissue situated between the outer wall of the myocardium and the visceral layer of the pericardium. EAT volumes were calculated by summation of EAT volume of each slice using the modified Simpson rule. Total RV volume (TRVV) was defined as RV end-diastolic volume + RV mass, and total ventricular heart volume (THV) was defined as TRVV + LV end-diastolic volume + LV mass + EAT volume. LV eccentricity index in end-diastole and end-systole was calculated as the ratio of the anterior-inferior and septal-posterolateral LV cavity dimensions in the

TABLE 3 Correlation and Partial Correlation of EAT

	All Patients				Nonobese Patients				Obese Patients			
	Correlation		Partial Correlation		Correlation		Partial Correlation		Correlation		Partial Correlation	
	r	*P* Value	r	*P* Value	r	*P* Value	r	*P* Value	r	*P* Value	r	*P* Value
LV GLS	0.28	<0.001	0.19	0.02	0.18	0.11	0.08	0.52	0.32	0.005	0.27	0.02
RV FWLS	0.16	0.04	0.15	0.07	−0.02	0.86	−0.04	0.71	0.32	0.006	0.30	0.01

Partial correlation adjusted for age, sex, and BMI.
BMI = body mass index; EAT = epicardial adipose tissue; FWLS = free wall longitudinal strain; GLS = global longitudinal strain; LV = left ventricular; RV = right ventricular.

FIGURE 2 Kaplan-Meier Curves for BMI, EAT, and Adverse Events

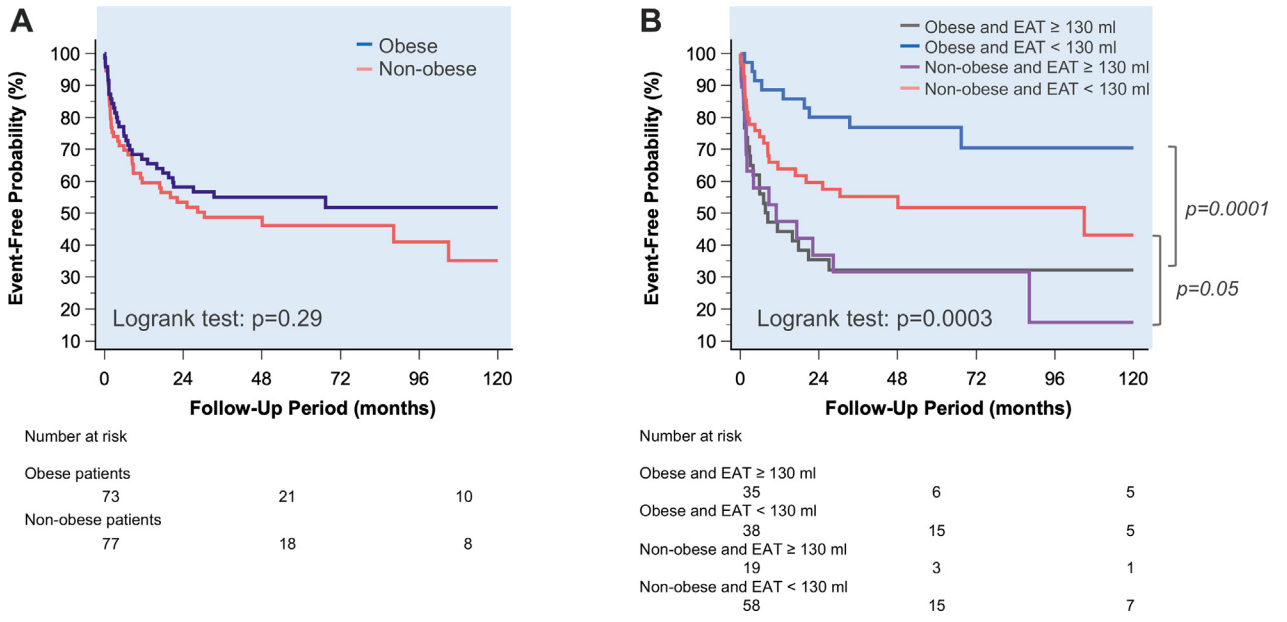

(A) Obese patients (BMI ≥ 30 kg/m^2) vs nonobese patients; (B) Integration of the optimal EAT cutoff value of 130 ml based on the area under ROC curve. BMI = body mass index; EAT = epicardial adipose tissue; ROC = receiver operating characteristics.

short-axis view at the mid-ventricular level. For feature-tracking analyses, LV short and long-axis (2-, 3-, and 4-chamber) cine were used to derive global radial strain, global circumferential strain, and global longitudinal strain. RV free wall longitudinal strain (RV FWLS) was determined from the 4-chamber view, and LA strain was from the long-axis 2- and 4-chamber cine images excluding the LA appendage. Endocardial and epicardial borders were manually drawn in the end-diastolic frame and then automatically propagated throughout the cardiac cycle by matching individual patterns that represent anatomical structures. The accuracy of the tracking was visually assessed and manually adjusted if necessary. On LGE images, the presence or absence of LGE was visually assessed. To evaluate inter- and intra-observer reproducibility, measurements of EAT and TRVV from a random sample of 10 HFpEF patients were independently assessed by 2 observers (S.N. and F.Y.), and 1 observer (S.N.) measured EAT and TRVV twice on 2 separate days with a washout period of at least 2 weeks.

CARDIAC PERFORMANCE AND ECHOCARDIOGRAPHIC ASSESSMENT. Brachial blood pressure (BP) and heart rate were measured during the CMR scan. All cardiac performance data were calculated from CMR-derived metrics. LV contractility was assessed using a single-beat Ees estimation algorithm developed by Chen et al.[22] Arterial afterload was determined as effective E_a (0.9·systolic BP/SV), systemic vascular resistance (mean BP/cardiac index·79.9), and total arterial compliance (SV/pulse pressure).[12] E_a/E_{es} ratio was used as an indicator of ventricular-arterial coupling.[23] Cardiac power output was defined as 0.222·cardiac output·mean BP/LV mass, where 0.222 is the conversion constant to W/100 g of LV myocardium.[24] Echocardiographic LV diastolic function was assessed using mean E/e' ratio. Estimated pulmonary artery systolic pressure was calculated from peak tricuspid regurgitation velocity and estimated right atrial pressure for the assessment of RV afterload.

OUTCOME ASSESSMENT. All subjects were followed up from the day of CMR assessment. The primary endpoint of this study was a composite of all-cause death or HF hospitalization. The HF hospitalization was defined as dyspnea and pulmonary edema on chest X-ray requiring intravenous diuretic treatment.

STATISTICAL ANALYSIS. Statistical analyses were performed using SPSS (version 25, IBM Inc) and R version 3.2.3. Continuous variables are expressed as mean ± SD or median (IQR) if not normally distributed and compared using an unpaired Student's t-test

FIGURE 3 Correlations Between Eccentric Index, EAT, and TRVV

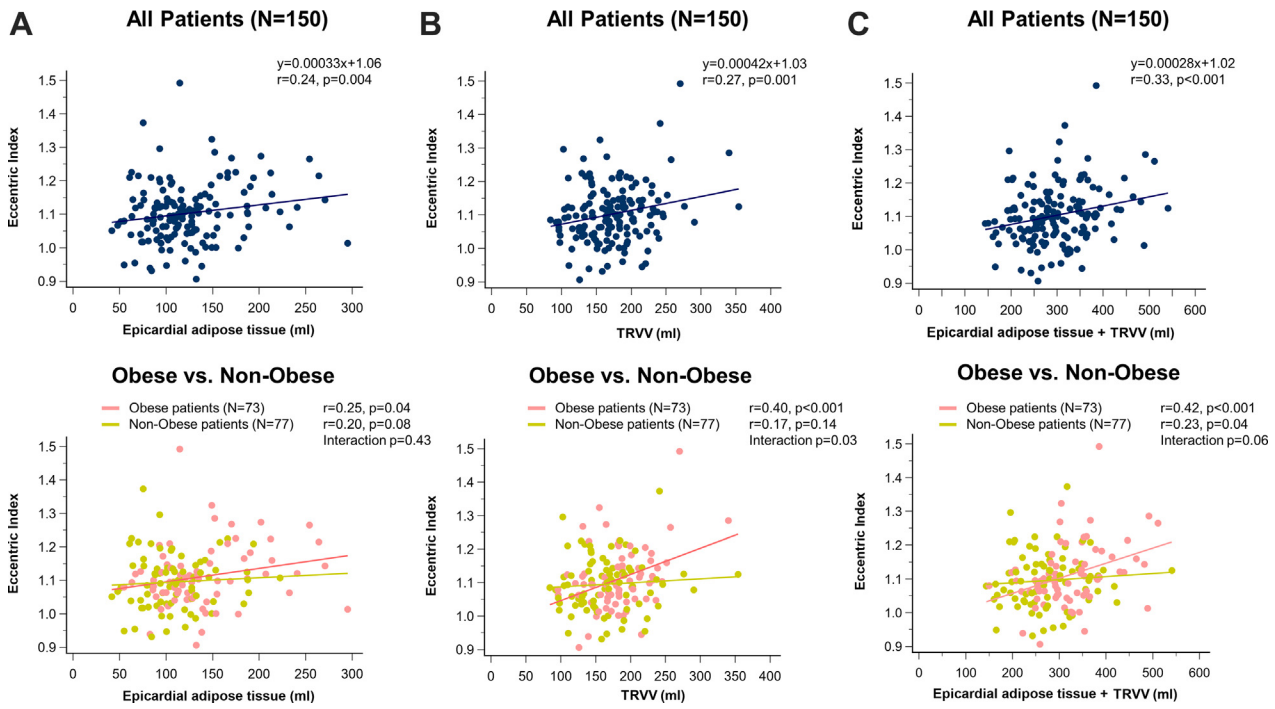

(A) Correlation of EAT to eccentric index; (B) Correlation of TRVV to eccentric index; and (C) Correlation of total amount of EAT and TRVV to eccentric index. These trends appear more profound in obese individuals, while there was no association in nonobese patients. EAT = epicardial adipose tissue; HFpEF = heart failure with preserved ejection fraction; TRVV = total right ventricular volume at end-diastole.

or Mann-Whitney nonparametric test as appropriate. Categorical variables were reported as counts and percentages and compared using a chi-squared test. The correlation between 2 variables was determined using Pearson's or Spearman's correlation coefficient and partial correlation coefficient. A partial correlation was controlled for age, sex, and body mass index (BMI). Simple linear regression analysis was used to assess the possible relationship of 2 variables in all patients. The area under the receiver operating characteristic was calculated and compared for all predictive tests for predicting the primary endpoint with a DeLong test. The Youden index was used to find the optimal predictive cut point for EAT and TRVV to improve diagnostic yield. Univariate and multivariate Cox regression models were used to estimate predictors of the primary endpoint adjusting for age, sex, and BMI. Kaplan-Meier curves were used to estimate the distribution of time to the first episode of HF admission or all-cause death. Differences between

TABLE 4 Correlation and Partial Correlation of Eccentric Index

	All Patients				Nonobese Patients				Obese Patients			
	Correlation		Partial Correlation		Correlation		Partial Correlation		Correlation		Partial Correlation	
	r	*P* Value	r	*P* Value	r	*P* Value	r	*P* Value	r	*P* Value	r	*P* Value
EAT	0.18	0.03	0.24	0.004	0.06	0.59	0.20	0.08	0.22	0.06	0.25	0.04
TRVV	0.22	0.01	0.27	0.001	0.07	0.53	0.17	0.14	0.36	0.002	0.40	<0.001
EAT + TRVV	0.24	0.003	0.33	<0.001	0.08	0.49	0.23	0.04	0.36	0.002	0.42	<0.001

Partial correlation adjusted for age, sex, and BMI.
BMI = body mass index; EAT = epicardial adipose tissue; TRVV = total right ventricular volume.

FIGURE 4 Representative Cases

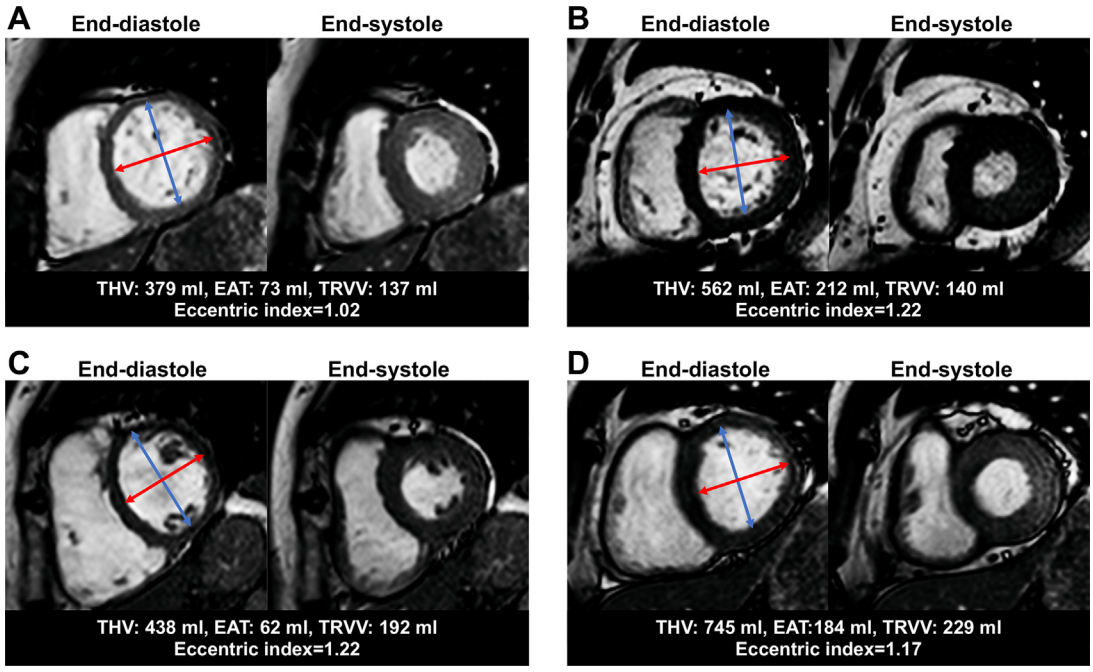

(A) Normal eccentric index without increased EAT and TRVV; (B) High eccentric index with increased EAT and normal TRVV; (C) High eccentric index with Increased TRVV and no increased EAT; (D) High eccentric index with increased EAT and TRVV. EAT = epicardial adipose tissue; THV = total heart volume; TRVV = total right ventricular volume at end-diastole.

time-to-event curves were compared with the log-rank test. Intra- and inter-observer reliability of EAT and TRVV measurements were assessed with the intraclass correlation coefficient. All tests were 2-sided, and a P value <0.05 was considered significant.

RESULTS

PATIENT POPULATION. Baseline clinical characteristics of the groups are summarized in Table 1. A total of 204 patients with HFpEF were identified, 54 of whom (obesity, n = 16; nonobesity, n = 38) were excluded (16 patients had cardiac amyloidosis, 5 had hypertrophic cardiomyopathy, 13 had pericardial effusion, 15 had insufficient short-axis slices, and 5 had poor image quality). Obese patients (BMI ≥30 kg/m^2) were younger, often felt shortness of breath, and had higher prevalence of obstructive sleep apnea and higher usage of diuretics. Irrespective of obesity stratification, the cohort was similar by sex, race, history of ischemic heart disease, hypertension, diabetes mellitus, dyslipidemia, and mild valvular heart disease. There was a trend for longer QRS duration and QTc duration in obese patients. There was no significant difference in laboratory parameters between both groups, despite a slight hemoconcentration in obese patients. The risk of HF admission was similar between groups, while there was a trend toward decreased mortality in obese HFpEF patients.

Table 2 summarizes rest hemodynamic parameters and CMR findings of study participants. Obese patients had greater stroke work and a trend toward higher systolic and diastolic resting BP; however, E_{es}, E_a, E_a/E_{es}, systemic vascular resistance, arterial compliance, and cardiac power output were comparable between groups. Obese patients had higher LV mass as well as SV and a trend of larger LV end-diastolic volume, indicative of increased concentricity with increased end-diastolic volume (both thick and dilated hypertrophy). Obese patients displayed significantly higher EAT, TRVV, and THV compared with nonobese patients, and the trends appeared more pronounced in obese patients with

FIGURE 5 ROC Curves for Adverse Outcomes in Obese (BMI ≥30 kg/m^2) and Nonobese Cohorts

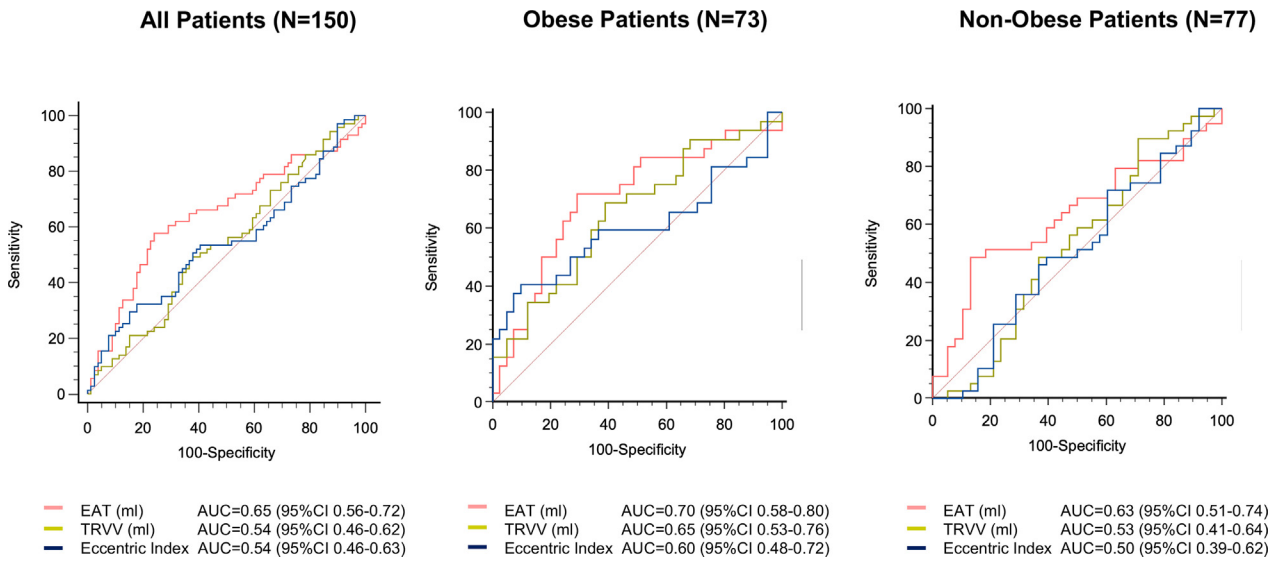

BMI = body mass index; EAT = epicardial adipose tissue; TRVV = total right ventricular volume at end-diastole.

suspected high-output HF defined as being >8 L/min, while there were no differences in eccentric index, atrial dimensions, and all echocardiographic parameters.

EAT FOR SUBCLINICAL CARDIAC REMODELING PARAMETERS, CARDIAC PERFORMANCE AND RISK STRATIFICATION. EAT had only a mild correlation with BMI (r = 0.37, $P < 0.001$), and male patients had higher EAT than female after adjusting BMI. LV global longitudinal strain as well as RV FWLS as subclinical cardiac remodeling parameters mildly correlated with EAT after controlling for age, sex, and BMI (partial correlation coefficient, r = 0.19, $P = 0.02$ and r = 0.15, $P = 0.07$, respectively), especially in the obese cohort (partial correlation coefficient, r = 0.27, $P = 0.02$ and r = 0.30, $P = 0.01$, respectively) (Figure 1, Table 3). In addition, impaired LA strain was likely to be associated with increased EAT (r = −0.13, $P = 0.11$). Regarding hemodynamic parameters, EAT mildly and negatively correlated with E_{es}, E_a, and systemic vascular resistance (r = −0.19, r = −0.26, r = −0.29, all $P < 0.05$) and positively correlated with arterial compliance and stroke work (r = 0.29 and 0.36, all $P < 0.01$). EAT was associated with a composite outcome in all patients (HR per 10 ml increase 1.06 [95% CI: 1.01-1.10], $P = 0.01$), and the association remained significant after adjusting age, sex, and BMI (HR per 10 ml increase 1.09 [95% CI: 1.04-1.15], $P < 0.001$). The EAT quantification provided improved risk stratification in predicting the primary endpoint in both obese and nonobese HFpEF patients. Kaplan-Meier curves showed the lowest risk of the primary composite outcome in obese patients without increased EAT (Figure 2).

ASSOCIATION AMONG EAT, TRVV AND ECCENTRIC INDEX. A significant correlation existed between EAT and TRVV (r = 0.35, $P < 0.001$). Even after adjusting for age, sex, increased BMI, and RV afterload, the association remained significant ($P < 0.001$). Figure 3 demonstrates the associations between end-diastolic eccentric index, EAT, and TRVV. Integrated assessment of EAT and TRVV are more closely associated with eccentric index than when either variable was used individually even after adjusting age, sex, and BMI (partial correlation coefficient, r = 0.33, $P < 0.001$) (Table 4). This trend appeared more profound in obese individuals. THV is also mildly correlated with eccentric index (partial correlation coefficient, r = 0.18, $P = 0.03$). Figure 4 and Videos 1 to 4 depict a case with normal end-diastolic eccentric index and several representative cases with high end-diastolic eccentric index. The intraclass correlation coefficients for interobserver and intraobserver measurements of EAT and TRVV were 0.93 (95% CI:

FIGURE 6 Kaplan-Meier Curves for EAT, TRVV, and Adverse Events

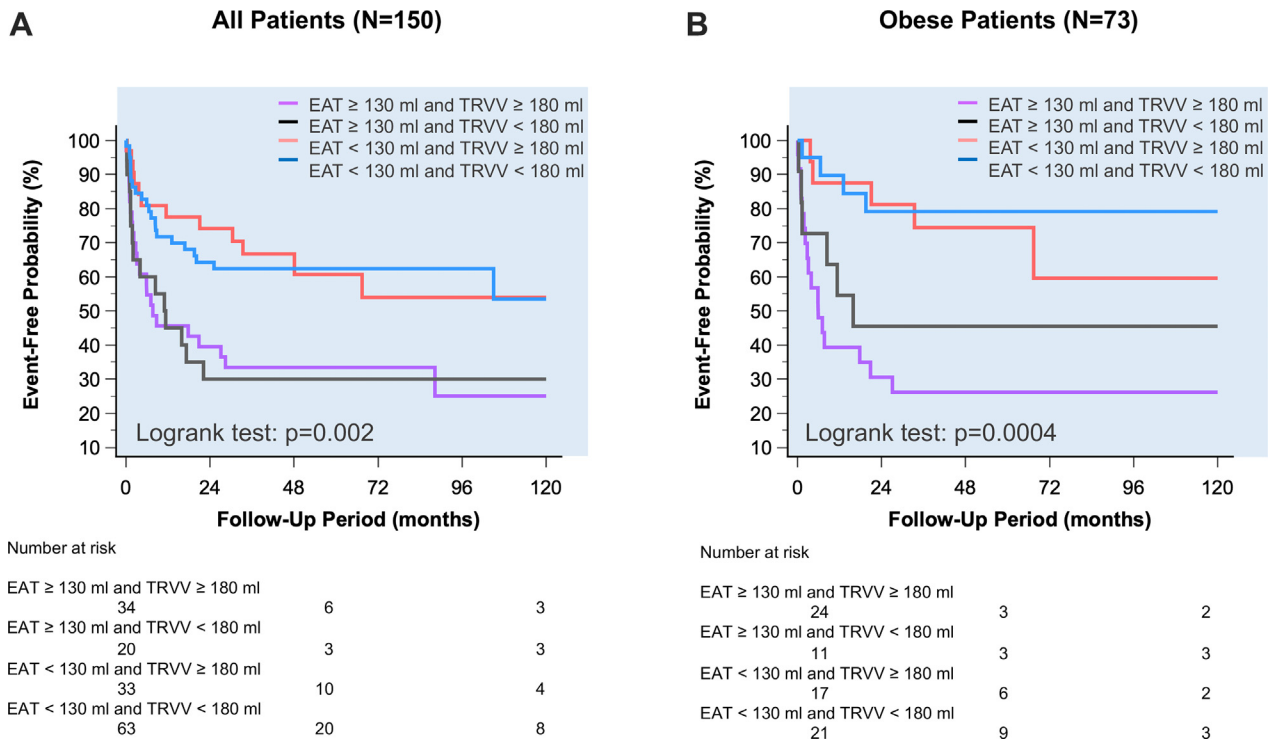

(A) All HFpEF patients; (B) Obese patients (BMI ≥30 kg/m^2). BMI = body mass index; EAT = epicardial adipose tissue; TRVV = total right ventricular volume at end-diastole.

0.77-0.98), 0.97 (95% CI: 0.87-0.99), 0.93 (95% CI: 0.75-0.98), and 0.96 (95% CI: 0.86-0.99), respectively.

EAT AND RV QUANTIFICATION FOR OBESE HFpEF PATIENTS. The C-statistic of EAT, TRVV, and end-diastolic eccentric index for predicting the primary endpoint in all patients were 0.65 (95% CI: 0.56-0.72), 0.54 (95% CI: 0.46-0.62) and 0.54 (95% CI: 0.46-0.63), respectively. However, the C-statistic of TRVV and end-diastolic eccentric index in the obese group was 0.65 (95% CI: 0.53-0.76) and 0.60 (95% CI: 0.48-0.72), respectively, which were greater compared with those of nonobese subgroup. Besides, there was a trend toward higher C-statistic of EAT in the obese subgroup (Figure 5). The integration of RV quantification into EAT provided an improved risk stratification with a C-statistic of 0.79 (95% CI: 0.67-0.90, DeLong test; $P = 0.09$) in obese patients. Figure 6 shows Kaplan-Meier curves stratified by EAT and TRVV in all patients and obese patients. Obese patients with EAT <130 ml and TRVV <180 ml had low risk (annual event rate 3.2%), while those with increased EAT ≥130 ml and TRVV ≥180 ml had significantly higher risk (annual event rate 11.8%; $P = 0.0004$) (Central Illustration).

DISCUSSIONS

In this retrospective study of 150 HFpEF patients referred for CMR, we demonstrate that: 1) increased EAT is closely associated with reduced RV and LV strain parameters, and the associations appear to be more pronounced in obese (BMI ≥30 kg/m^2) patients; 2) EAT is the important predictor of HF admission and all-cause death regardless of obesity, and correlates with TRVV even after adjusting for increased BMI and RV afterload; 3) integrated assessments of EAT and TRVV more closely match LV end-diastolic eccentric index in obese patients; and 4) quantification of EAT and RV structure provides additive risk stratification for adverse outcomes in obese HFpEF.

Given RV dysfunction rather than LV is a pivotal process associated with adverse outcome and a potential therapeutic target in HFpEF patients,[25] an improved understanding of RV remodeling including extracardiac structures, may be of great importance and facilitate the development of newer HF therapies.

CENTRAL ILLUSTRATION New Risk-Stratification in Obese HFpEF Patients Using EAT and RV Quantification

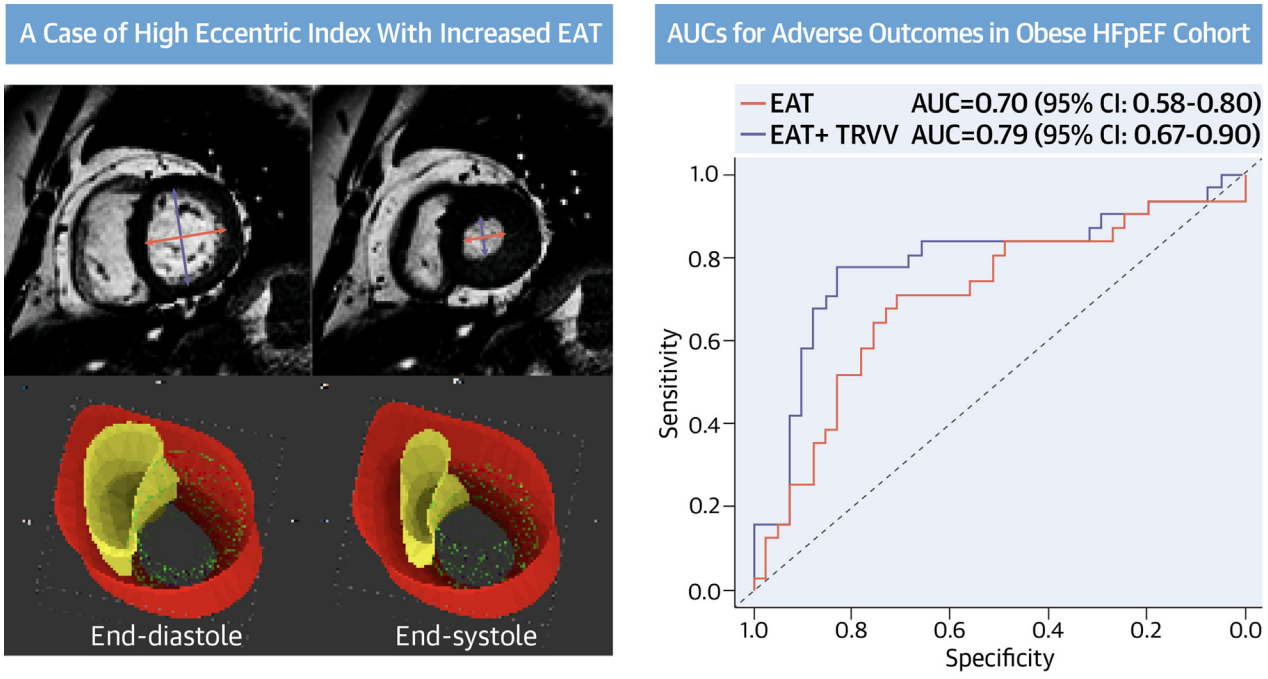

Nakamori S, et al. JACC Adv. 2023;2(10):100730.

EAT = epicardial adipose tissue; TRVV = total right ventricular volume at end-diastole.

In accordance with previous studies,[15,16] the results in the present study demonstrated larger TRVV in obese HFpEF. Also, larger TRVV was closely associated with EAT even after adjusting increased BMI and RV afterload. Interestingly, EAT mildly correlated with reduced RV FWLS, and the correlation of EAT and RV FWLS appeared to be more profound in obese HFpEF, which implies a clinical importance for the accurate assessment of RV function and morphology and EAT quantification by CMR. This finding may reflect the presence of other subclinical conditions, such as postcapillary pulmonary hypertension or RV ischemia that affect RV function in patients with obesity. However, we found no significant associations between TRVV, RV FWLS, and RV afterload, while there were correlations between RV ejection fraction, RV end-systolic volume, and RV afterload. This observation suggests that the effect of EAT on RV remodeling may outweigh other pathogenic effects in obese HFpEF patients. Therefore, besides the treatment of RV afterload, it seems important to lower BMI or target the EAT reduction to alter further adverse hemodynamics or myocardial remodeling in an earlier stage of obese HFpEF. Comprehensive assessment of EAT and RV structure broadens our understanding of mechanisms that underlie progression of RV remodeling in HFpEF and might help provide more precise phenotyping of HFpEF.

Studies have reported that heightened ventricular interdependence as well as increased pericardial restraint is an important contributor to LV filling pressures in HF.[12,19,26,27] This distinction is of critical importance to guide treatment decision in obese HFpEF patients. Right atrial pressure is considered a reliable estimate of pericardial pressure and is used to assess the degree of relative pericardial restraint. However, in a study by Tyberg et al,[28] there was a difference between right atrial pressure and pericardial pressure in the case with dilated RV cavity, suggesting its limited diagnostic accuracy especially in obese HFpEF patients. Eccentric index, which is quantified from a short-axis view, is also a useful indicator of ventricular interdependence.[29] Our study results are consistent with the study by Koepp et al[26] showing that 2D transthoracic echo eccentric index at end-diastole and end-systole is higher in obese HFpEF patients with increased EAT. However, selection of imaging planes and accuracy of 2D echo are dependent on operator experience, and limited acoustic windows may not allow accurate short-axis views of the heart. We found important variability of differences in eccentric index of each slice even in the same patient (Supplemental Figure 1). Thus, relatively small measurement errors can lead to some differences in eccentric index value. In obese HFpEF cohort, integration of RV quantification to EAT were closely associated with eccentric index at end-diastole and provided improved risk stratification for adverse outcomes beyond eccentric index. These findings would support the potential of comprehensive assessment of EAT and TRVV as an alternative marker of eccentric index for assessment of ventricular interdependence. In addition, an increased pericardial pressure can also be caused by accumulation of EAT as well as alteration of the inherent properties of the pericardium such as inflammation and fibrosis. Different from dilated cardiomyopathy or severe bi-atrial enlargement from permanent atrial fibrillation with valvular heart disease, where the total epicardial volume enlargement and resultant relative pericardial restraint occur, understanding the relationship between EAT, TRVV, and left-side filling pressures has important clinical implications in the management of obese HFpEF patients.

STUDY LIMITATIONS. Our study has several limitations. It is a single-center, retrospective study with a relatively small sample size. We studied patients referred for CMR spanning a period of 10 years. HF management might have changed over the course of the study. However, it does not mean that CMR metrics are modifiable. Also, these are resting CMR metrics, and so there might not be significant relationships on intracardiac pressure and other hemodynamics. Hemodynamic assessments with EAT and TRVV might be more evident with exercise parameters and could be looked at in other studies.

CONCLUSIONS

In obese HFpEF, increased EAT correlated with impaired RV longitudinal strain after controlling for RV afterload, and increased amount of EAT and TRVV was associated with greater LV end-diastolic eccentric index. CMR quantification of EAT and RV structure provides insight into HFpEF heterogeneous pathophysiology and allows for improved risk stratification for adverse outcomes in obese patients with HFpEF.

FUNDING SUPPORT AND AUTHOR DISCLOSURES

Dr Nezafat has received grant funding from the National Institutes of Health (NIH) grants R01 HL127015, R01 HL129157, R01 HL129185, R01 HL154744, R01 HL158098, and R01 HL129185. All other authors have reported that they have no relationships relevant to the contents of this paper to disclose.

ADDRESS FOR CORRESPONDENCE: Dr Reza Nezafat, Cardiovascular Division, Department of Medicine, Beth Israel Deaconess Medical Center, 330 Brookline Ave, Boston, Massachusetts 02215, USA. E-mail: rnezafat@bidmc.harvard.edu.

PERSPECTIVES

COMPETENCY IN MEDICAL KNOWLEDGE: In obese HFpEF, increased EAT correlated with impaired RV longitudinal strain after controlling for RV afterload, and increased amount of EAT and TRVV was associated with greater LV end-diastolic eccentric index. The integration of RV quantification into EAT provided improved risk stratification for adverse outcomes in obese HFpEF.

TRANSLATIONAL OUTLOOK: We assessed whether EAT and RV quantification using CMR would provide a better understanding of obesity-related pathophysiology and improve risk stratification in obese patients with HFpEF. Further studies are warranted to confirm the potential of comprehensive assessment of EAT and TRVV as an alternative marker of eccentric index for assessment of ventricular interdependence.

REFERENCES

1. Paulus WJ, Tschöpe C, Sanderson JE, et al. How to diagnose diastolic heart failure: a consensus statement on the diagnosis of heart failure with normal left ventricular ejection fraction by the Heart Failure and Echocardiography Associations of the European Society of Cardiology. *Eur Heart J*. 2007;28:2539–2550.

2. Borlaug BA, Paulus WJ. Heart failure with preserved ejection fraction: pathophysiology, diagnosis, and treatment. *Eur Heart J*. 2011;32:670–679.

3. Sharma K, Kass DA. Heart failure with preserved ejection fraction: mechanisms, clinical features, and therapies. *Circ Res*. 2014;115:79–96.

4. Reddy YNV, Borlaug BA. Heart failure with preserved ejection fraction. *Curr Probl Cardiol*. 2016;41:145–188.

5. Owan TE, Hodge DO, Herges RM, Jacobsen SJ, Roger VL, Redfield MM. Trends in prevalence and outcome of heart failure with preserved ejection fraction. *N Engl J Med*. 2006;355:251–259.

6. Pfeffer MA, Claggett B, Assmann SF, et al. Regional variation in patients and outcomes in the treatment of preserved cardiac function heart failure with an aldosterone antagonist (TOPCAT) trial. *Circulation*. 2015;131:34–42.

7. Solomon SD, McMurray JJV, Anand IS, et al. Angiotensin-neprilysin inhibition in heart failure with preserved ejection fraction. *N Engl J Med*. 2019;381:1609–1620.

8. Shah SJ, Kitzman DW, Borlaug BA, et al. Phenotype-specific treatment of heart failure with preserved ejection fraction. *Circulation*. 2016;134:73–90.

9. Lindman BR, Dávila-Román VG, Mann DL, et al. Cardiovascular phenotype in HFpEF patients with or without diabetes: a RELAX trial ancillary study. *J Am Coll Cardiol*. 2014;64:541–549.

10. Samson R, Jaiswal A, Ennezat PV, Cassidy M, Le Jemtel TH. Clinical phenotypes in heart failure with preserved ejection fraction. *J Am Heart Assoc*. 2016;5:1–15.

11. Borlaug BA, Obokata M. Is it time to recognize a new phenotype? heart failure with preserved ejection fraction with pulmonary vascular disease. *Eur Heart J*. 2017;38(38):2874–2878.

12. Obokata M, Reddy YNV, Pislaru SV, Melenovsky V, Borlaug BA. Evidence supporting the existence of a distinct obese phenotype of heart failure with preserved ejection fraction. *Circulation*. 2017;136:6–19.

13. Kresoja KP, Rommel KP, Wachter R, et al. Proteomics to improve phenotyping in obese patients with heart failure with preserved ejection fraction. *Eur J Heart Fail*. 2021;23:1633–1644.

14. Redfield MM, Chen HH, Borlaug BA, et al. Effect of phosphodiesterase-5 inhibition on exercise capacity and clinical status in heart failure with preserved ejection fraction: a randomized clinical trial. *JAMA*. 2013;309:1268–1277.

15. Chahal H, McClelland RL, Tandri H, et al. Obesity and right ventricular structure and function: the MESA-right ventricle study. *Chest*. 2012;141:388–395.

16. Wong CY, O'Moore-Sullivan T, Leano R, Hukins C, Jenkins C, Marwick TH. Association of subclinical right ventricular dysfunction with obesity. *J Am Coll Cardiol*. 2006;47:611–616.

17. Mazurek T, Zhang L, Zalewski A, et al. Human epicardial adipose tissue is a source of inflammatory mediators. *Circulation*. 2003;108:2460–2466.

18. van Woerden G, van Veldhuisen DJ, Manintveld OC, et al. Epicardial adipose tissue and outcome in heart failure with mid-range and preserved ejection fraction. *Circ Heart Fail*. 2022;15:e009238.

19. Borlaug BA, Reddy YNV. The role of the pericardium in heart failure: implications for pathophysiology and treatment. *J Am Coll Cardiol HF*. 2019;7:574–585.

20. Ponikowski P, Voors AA, Anker SD, et al. 2016 ESC guidelines for the diagnosis and treatment of acute and chronic heart failure: the Task Force for the diagnosis and treatment of acute and chronic heart failure of the European Society of Cardiology (ESC) developed with the special contribution of the Heart Failure Association (HFA) of the ESC. *Eur Heart J*. 2016;37:2129–2200.

21. Heidenreich PA, Bozkurt B, Aguilar D, et al. 2022 AHA/ACC/HFSA guideline for the management of heart failure: a report of the American College of Cardiology/American Heart Association Joint Committee on clinical practice guidelines. *J Am Coll Cardiol*. 2022;79:e263–e421.

22. Chen CH, Fetics B, Nevo E, et al. Noninvasive single-beat determination of left ventricular end-systolic elastance in humans. *J Am Coll Cardiol*. 2001;38:2028–2034.

23. Ky B, French B, May Khan A, et al. Ventricular-arterial coupling, remodeling, and prognosis in chronic heart failure. *J Am Coll Cardiol*. 2013;62:1165–1172.

24. Anand V, Kane GC, Scott CG, et al. Prognostic value of peak stress cardiac power in patients with normal ejection fraction undergoing exercise stress echocardiography. *Eur Heart J*. 2021;42:776–785.

25. Obokata M, Reddy YNV, Melenovsky V, Pislaru S, Borlaug BA. Deterioration in right ventricular structure and function over time in patients with heart failure and preserved ejection fraction. *Eur Heart J*. 2019;40:689–697.

26. Koepp KE, Obokata M, Reddy YNV, Olson TP, Borlaug BA. Hemodynamic and functional impact of epicardial adipose tissue in heart failure with preserved ejection fraction. *J Am Coll Cardiol HF*. 2020;8:657–666.

27. Maniar HS, Prasad SM, Gaynor SL, Chu CM, Steendijk P, Moon MR. Impact of pericardial restraint on right atrial mechanics during acute right ventricular pressure load. *Am J Physiol Heart Circ Physiol*. 2003;284:H350–357.

28. Tyberg JV, Taichman GC, Smith ER, Douglas NW, Smiseth OA, Keon WJ. The relationship between pericardial pressure and right atrial pressure: an intraoperative study. *Circulation*. 1986;73:428–432.

29. Ryan T, Petrovic O, Dillon JC, Feigenbaum H, Conley MJ, Armstrong WF. An echocardiographic index for separation of right ventricular volume and pressure overload. *J Am Coll Cardiol*. 1985;5:918–927.

KEY WORDS cardiovascular magnetic resonance, epicardial adipose tissue, heart failure with preserved ejection fraction, right ventricular quantification

APPENDIX For supplemental videos and figures, please see the online version of this paper.